Supplementary information:
Exploring the impact of select anchor groups for norbornadiene/quadricyclane single-molecule switches

Shima Ghasemi,[a] Luca Ornago,[b] Zacharias Liasi,[c] Magnus Bukhave Johansen,[c] Theo Juncker von Buchwald,[c] Andreas Erbs Hillers-Bendtsen,[c] Sebastiaan van der Poel,[b] Helen Hölzel,[d] Zhihang Wang,[h] Francoise M. Amombo Noa,[a] Lars Öhrström,[a] Kurt V. Mikkelsen, [c] Herre S. J. van der Zant, [b] Samuel Lara-Avila,[g] and Kasper Moth-Poulsen[*adef]

[a] Department of Chemistry and Chemical Engineering, Chalmers University of Technology, SE-412 96 Gothenburg, Sweden.

[b] Kalvi Institute of Nanoscience, Delft University of Technology, NL-2628 CJ Delft, The Netherlands.

[c] Department of Chemistry, University of Copenhagen, DK-2100 Copenhagen Ø, Denmark.

[d] Department of Chemical Engineering, Universitat Politècnica de Catalunya, EEBE, ES-08019 Barcelona, Spain.

[e] Catalan Institution for Research and Advanced Studies, ICREA, ES-08010 Barcelona, Spain

[f] The Institute of Materials Science of Barcelona, ICMAB-CSIC, ES-08193 Barcelona, Spain.

[g] Department of Microtechnology and Nanoscience, Chalmers University of Technology, SE-412 96 Gothenburg, Sweden

[h] Department of Materials Science and Metallurgy, University of Cambridge, 27 Charles Babbage Rd, Cambridge CB3 0FS, U.K.

Email: kasper.moth-poulsen@chalmers.se

Contents

1. Synthesis and characterization

General procedures: Starting materials were purchased from Sigma Aldrich and Fisher Scientific. All reactions were performed under a nitrogen atmosphere using oven-dried glassware. Products were characterized by proton (^{1}H) and carbon (^{13}C) nuclear magnetic resonance (NMR) spectroscopy using an automated Agilent (Varian) 400 MHz spectrometer and a Bruker 700 MHz Avance III 4-channel spectrometer equipped with a 5 mm QCI cryoprobe and a SampleJet sample changer. Mass spectrophotometer was micrOTOF-Q II Bruker (flight time analyzer), Bruker and the recording was made with positive polarity.

Dry solvents (toluene and tetrahydrofuran) were obtained from a MBraun MB SPS-800 solvent purification system. Purification through column chromatography was carried out using a Biotage Isolera™ system.

a. *p*-Toluenesulfonyl Bromide (**2**)
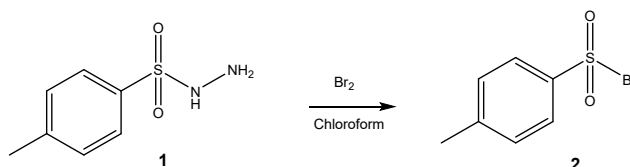
p-Toluenesulfonyl hydrazide (50 g, 0.27 mol) was added to a flask containing CHCl$_3$ (500 mL) at 0 °C. Bromine (27 mL, 0.54 mol) was slowly added dropwise to the solution. (Caution: When the temperature of the mixture rose above 0° C, small amounts of ice were added to maintain the temperature). After the addition of the final portion of bromine, the mixture remained white in color. A small amount of additional bromine was added until a light orange color persisted. The organic phase was then separated from the aqueous phase, and the organic phase was washed with saturated aqueous NaHCO$_3$ solution (2 × 100 mL) and 1% aqueous Na$_2$S$_2$O$_3$ solution (2 × 100 mL). The organic phase was dried over Na$_2$SO$_4$, filtered, and the solvent was evaporated to yield the product as a white solid (yield: 95%). Experimental data corroborated with literature reports.[1]

b. 2,3-Dibromonorbornadiene (**4**)
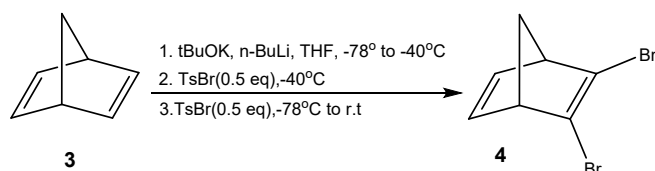
Potassium *tert*-butoxide (11.2 g, 0.1 mol) was weighed inside a glove box and dissolved in THF (200 mL). The solution was cooled to -84 °C, and liquid nitrogen was continuously added to ethyl acetate to maintain a stable temperature of -84 °C during the reaction. Then, norbornadiene (12.2 mL, 0.12 mol) was added to the mixture, followed by the dropwise addition of *n*-BuLi (2.5 M in hexane, 40 mL, 0.1 mol) over 60 minutes. After stirring for an additional 15 minutes at -84 °C, the mixture was transferred to -41 °C (using an acetonitrile/liquid N2 bath) and stirred for 60 minutes. Subsequently, the solution

was cooled back to -84 °C, and *p*-toluenesulfonyl bromide (**2**) (11.7 g, 0.05 mol) was added to the reaction mixture in portions under a nitrogen atmosphere. The mixture was stirred for 15 minutes at -84 °C, and then transferred to a -41 °C bath for one hour.

In the last step, the solution was again cooled to -84 °C, and *p*-toluenesulfonyl bromide (11.7 g, 0.05 mol) was added to the mixture. After stirring at this temperature for 15 minutes, the reaction mixture was kept at ambient temperature for one hour. The reaction was quenched by adding water (50 mL), and the product was extracted with diethyl ether (2 × 50 mL). The solution was dried over MgSO$_4$, and the solvent was evaporated under vacuum, resulting in a brown crude product. The crude product was dissolved in pentane (50 ml), washed with deionized water (2 × 100 mL) and brine (50 mL) dried over MgSO$_4$, and filtered. The solvent was then removed under vacuum to obtain a red solution. The product was further purified by distillation using a short Vigreux column. Firstly, the mono norbornadiene fraction was collected at 30-50 °C and 5×10^{-2} mbar. Finally, the 2,3-dibromonorbornadiene product (**4**) was collected at 90-100 °C as a colorless liquid. The product was stored in a -80 °C freezer to prevent possible degradation. (Yield: 16%), ^{1}H-NMR (400 MHz, CDCl$_3$) δ (ppm) = 6.88 (m, 1H), 3.62 (m, 1H), 2.45 (dt, 1H), 2.18 (dt, 1H). Experimental data were consistent with literature reports.[1]

c. (4-Bromo) phenyl-tert-butylthioether (**6**)
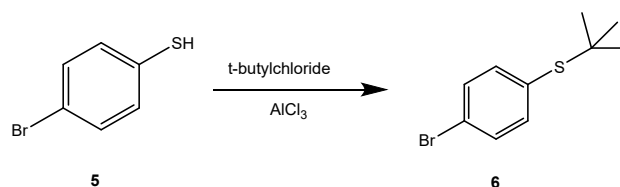
4-Bromothiophenol (5 g, 26.5 mmol) was added to 2-chloro-2-methylpropane (20 mL) in a flask. Subsequently, aluminum chloride (175 mg, 1.3 mmol) was added in small portions at room temperature. After one hour, the solution turned bright orange. The reaction mixture was quenched with water (100 mL) and extracted with *n*-pentane (3 × 50 mL), then washed with brine (50 mL). The solution was dried over anhydrous MgSO$_4$, and the solvent was removed under reduced pressure. The crude product was purified using column chromatography (*n*-pentane) to yield 90% as a colorless oil.

The ^{1}H-NMR spectrum (CDCl$_3$, 400 MHz) displayed the following peaks: δ (ppm) = 7.46-7.37 (m, 4H), 1.27 (s, 9H). The experimental data obtained were consistent with literature reports.[2]

d. 1-*tert*-Butylthio-4-[(trimethylsilyl)ethynyl] benzene (**8**)
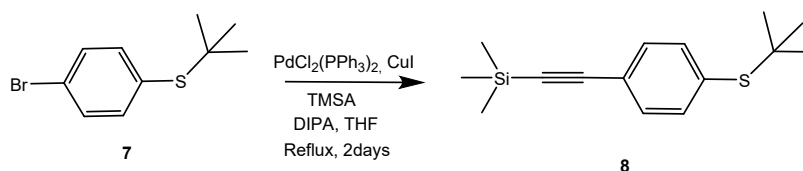
In an oven-dried two-neck flask, dichlorobis(triphenylphosphine)palladium(II) (287 mg, 0.408 mmol) and copper iodide (104 mg, 0.543 mmol) were added to THF (50 mL) and degassed with argon gas for one hour. After adding **7** (2.00 g, 8.16 mmol) and trimethylsilylacetylene (1.42 g, 14.5 mmol), the solution changed color from orange to red. In the final step, diisopropylamine (2.4 mL) was added to the reaction mixture, resulting in a dark brown color. The reaction was refluxed for 48 hours, the mixture was poured into water (100 mL). The resulting mixture was extracted with ether (3 x 30 mL), and the organic phase was washed with brine (100 mL). The organic layer was dried over sodium sulfate

(Na$_2$SO$_4$), filtered, and the solvent was removed by rotary evaporation, leaving a black residue. The crude product was purified by column chromatography using hexane, yielding 58% as a yellow liquid. ^{1}H-NMR (CDCl$_3$, 400 MHz): δ (ppm) = 7.47-7.40 (m, 4H), 1.27 (s, 9H), 0.25 (s, 9H). Data according to the literature.[3]

e. 1-*tert*-Butylthio-4-ethynylbenzene (**10**)
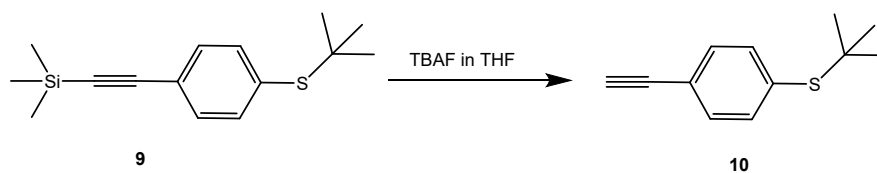
A solution of **9** (1.1 g, 4.18 mmol) in THF (15 mL) was cooled to 0 °C and degassed with argon gas for 30 minutes. Subsequently, TBAF (2.3 g, 2.5 mL) was added dropwise to the reaction mixture under a nitrogen atmosphere. The reaction mixture was stirred for 30 minutes at 0 °C and then kept at room temperature for an additional two hours and thirty minutes. 1 g of silica was added to the reaction mixture. The silica was filtered from the reaction mixture, and the solvent was removed by rotary evaporation. The crude product was dissolved in dichloromethane (30 mL), washed with saturated aqueous sodium bicarbonate (3 x 50 mL), water (2 x 50 mL), and brine (50 mL), and dried over Na_2SO_4. After filtration and solvent removal, the product was obtained as a red liquid without further purification, the compound was used for the next step reaction(66% yield). ^{1}H-NMR (CDCl$_3$, 400 MHz): δ (ppm) = 7.50-7.43 (m, 4H), 3.14 (s, 1H), 1.29 (s, 9H). Data according to the literature.[3]

f. 2,3-bis((4-(*tert*-butylthio) phenyl) ethynyl)bicyclo[2.2.1]hepta-2,5-diene (**NBD-1**)
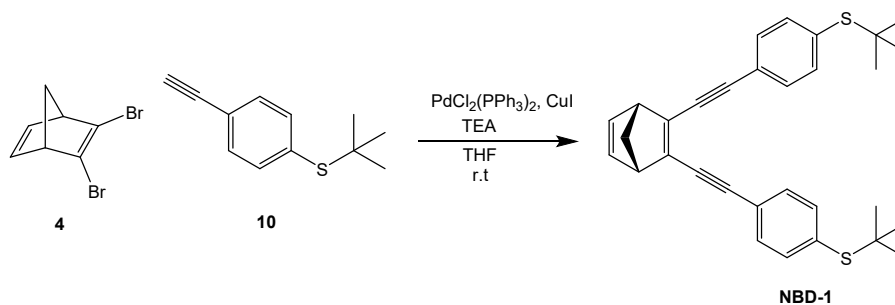
In an oven-dried two-neck flask, dichlorobis(triphenylphosphine)palladium(II) (14 mg, 0.02 mmol) and copper iodide (3.8 mg, 0.02 mmol) were placed in THF (5 mL). Subsequently, compound **4** (100 mg, 0.4 mmol) was added to the reaction mixture, and the solution was degassed with argon gas for 30 minutes. Next, a solution of compound **10** (152 mg, 0.8 mmol) in 2 mL dry THF was added, followed by the addition of triethylamine (0.8 mL, 6 mmol). The reaction mixture was refluxed for 20 hours and then poured into water (25 mL). The organic phase was extracted with dichloromethane (3 x 20 mL), and the organic layers were washed with water (3 x 50 mL) and brine (2 x 30 mL) and dried over Na_2SO_4. The solvent was removed under reduced pressure, resulting in yellow solid crude product. The crude product was purified by column chromatography using a mixture of hexane and dichloromethane (10:2) to yield the final product as a yellow solid with a 50% yield. ^{1}H-NMR (CDCl$_3$, 700 MHz): δ (ppm) = 7.50 (m, 4H), 7.43 (m, 4H), 6.88 (m, 2H), 3.79(dq, *J* = 3.3, 1.6 Hz, 2H), 2.32 (dt, *J* = 6.8, 1.6 Hz, 1H), 2.19 (dt, *J* = 6.8, 1.6 Hz, 1H), 1.29(s, 18H) ^{13}C-NMR (CDCl$_3$, 700 MHz): 141.96, 137.22, 133.38, 132.34, 131.26, 123.81, 102.89, 87.40, 71.45, 36.15, 46.57, 31.01. HRMS (ESI-TOF) m/z: [M + Na]$^+$ Calcd for $C_{31}H_{32}S_2Na$ 491.1838; Found 491.1814

g. Bicyclo [2.2.1] hepta-2,5-diene-2,3-diyl) bis(ethyne-2,1-diyl)) bis(4,1-phenylene)) diethanethioate (**NBD-2**)

NBD-1   NBD-2
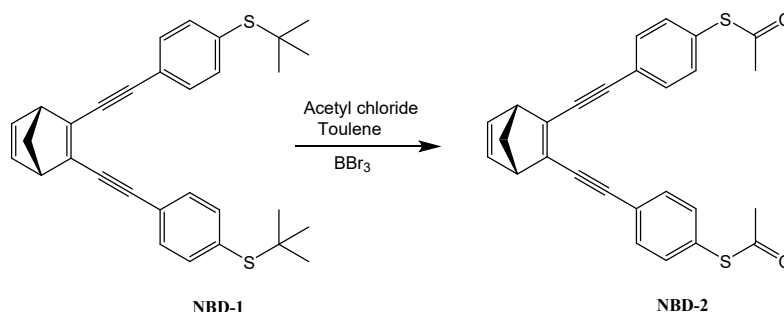
Compound **11** (210 mg, 0.44 mmol) was dissolved in toluene (15 mL). After the addition of acetyl chloride (0.13 mL), the mixture was degassed with argon gas for 30 minutes and cooled to 0 °C. A solution of BBr_3 in dichloromethane (DCM) (0.9 mL) was then added dropwise to the reaction mixture. The progress of the reaction was monitored by TLC, and after two hours, the mixture was transferred to a beaker containing ice. Once the mixture reached room temperature, it was extracted with DCM (3 x 20 mL), and the organic layers were washed with water (3 x 50 mL) and brine (2 x 30 mL), and dried over Na_2SO_4. The solvent was removed by rotary evaporation. The crude product was purified by column chromatography using a mixture of hexane and DCM (10:3) to yield the final product as a yellow solid with a 20% yield. The yellow crystals were collected from the final product after recrystallization in a mixture of hexane and DCM. ^{1}H NMR (700 MHz, $CDCl_3$) δ(ppm) = 7.53 – 7.47 (m, 4H), 7.41 – 7.35 (m, 4H), 6.88 (t, J = 1.9 Hz, 2H), 3.79 (dq, J = 3.3, 1.6 Hz, 2H), 2.43 (s, 6H), 2.32 (dt, J = 6.8, 1.6 Hz, 1H), 2.19 (dt, J = 6.8, 1.6 Hz, 1H).^{13}C-NMR ($CDCl_3$, 700 MHz): 193.43, 142.08, 141.91, 134.14, 131.89, 128.10, 124.60, 102.70, 87.42, 71.46, 56.07, 30.25. HRMS (ESI-TOF) m/z: [M + Na] [+] Calcd for $C_{27}H_{20}O_2S_2Na$ 463.0797; Found 463.0779.

h. Trimethyl((4-(methylthio) phenyl)ethynyl)silane (**12**)

11   12
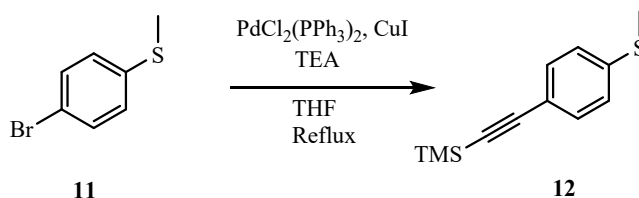
An oven-dried two-neck flask was prepared and charged with dichlorobis(triphenylphosphine) palladium(II) (27.5 mg, 0.038 mmol) and copper iodide (7.2 mg, 0.037 mmol) in THF (5 mL). Subsequently, compound **11** (0.4 g, 1.9 mmol) was added to the reaction mixture, and the solution was degassed for 30 minutes. In the next step, a solution of trimethylsilylacetylene (0.36 mL, 2.2 mmol) in 2 mL dry THF was added to the mixture, followed by the addition of triethylamine (3 mL). The reaction mixture was refluxed for 20 hours and then poured into water (25 mL). After extraction of the organic phase with dichloromethane (3 x 20 mL), the organic layers were washed with water (3 x 50 mL) and brine (2 x 30 mL) and dried over Na_2SO_4. The solvent was removed under reduced pressure to obtain

the crude product as a yellow solid. The crude product was purified by column chromatography using hexane, yielding the final product as a yellow oil with a 70% yield. ^{1}H-NMR (CDCl$_3$, 400 MHz): δ (ppm) = 7.38-7.16 (m, 4H), 2.48 (s, 3H), 0.24 (s, 9H). The data provided is in accordance with the literature.[4]

i. (4-ethynylphenyl)(methyl)sulfane (**14**)

13 **14**
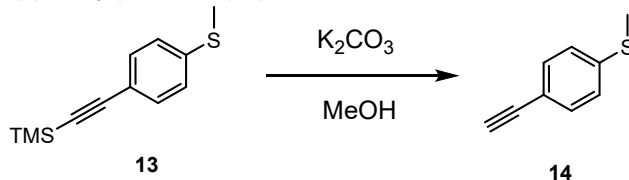
In a flask, compound **13** (0.8 g, 3.6 mmol) and potassium carbonate (0.8 g, 5 mmol) were dissolved in methanol (50 mL). The reaction mixture was stirred overnight. Upon completion of the reaction, which was monitored by TLC, the solution was diluted with water (100 mL) and extracted with ethyl acetate (3 x 20 mL). The organic layer was then washed with brine (100 mL) and dried using MgSO$_4$. The solvent was removed using a rotary evaporator, resulting in the formation of a pale-yellow oil product with a yield of 100%. ^{1}H-NMR (CDCl$_3$, 400 MHz): δ (ppm) = 7.38-7.16 (m, 4H), 3.01 (s, 1H), 2.48 (s, 3H). The provided data is consistent with the literature.[4]

j. Bis((4-(methylthio) phenyl)ethynyl)bicyclo[2.2.1]hepta-2,5-diene (**16**)

4 **14** **NBD-3**
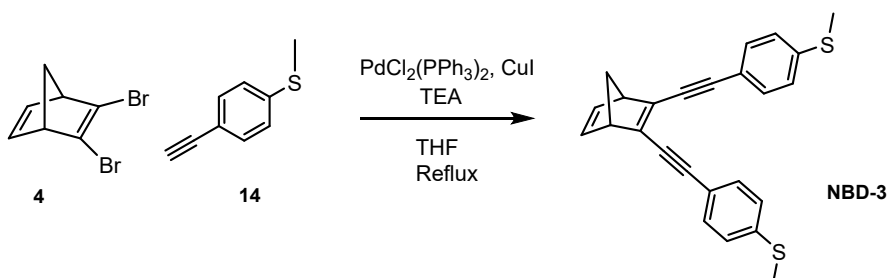
A two-neck oven-dried flask was charged with dichlorobis(triphenylphosphine)palladium (II) (14 mg, 0.02 mmol) and copper iodide (3.8 mg, 0.02 mmol) in THF (5 mL). Subsequently, compound **4** (100 mg, 0.4 mmol) was added to the reaction mixture and the solution was degassed for 30 min. In the next step, a solution of compound 14 (120 mg, 0.8 mmol) in 2 mL dry THF was added to the mixture and followed by adding triethylamine (0.8 mL, 6 mmol). The reaction mixture was refluxed for 20 hours and poured into water (25 mL). After extraction of the organic phase with dichloromethane (3 x20 mL), the organic layers were washed with water (3 x 50 mL), and brine (2 x 30 mL), and dried over Na$_2$SO$_4$. The solvent was removed under reduced pressure to afford the crude a yellow solid. The crude product was purified by column chromatography using Hexane/DCM (10:2) to give the final product as a yellow solid (40% yield). ^{1}H NMR (CDCl3, 700 MHz): δ(ppm) = 7.39 (m, 4H), 7.19 (m, 4H), 6.88 (m, 2H), 3.77(dq, J = 3.3, 1.6 Hz, 2H), 2.49 (s, 6H), 2.30 (dt, J = 6.8, 1.6 Hz, 1H), 2.17 (dt, J = 6.8, 1.6 Hz, 1H). ^{13}C NMR (CDCl$_3$, 700 MHz): 141.89, 141.25, 139.37, 131.59, 125.75, 119.77, 103.12, 86.18, 71.24, 56, 15.29. HRMS (ESI-TOF) m/z: [M + Na] $^+$ Calcd for C$_{25}$H$_{20}$S$_2$Na 407.0899; Found 407.0880.
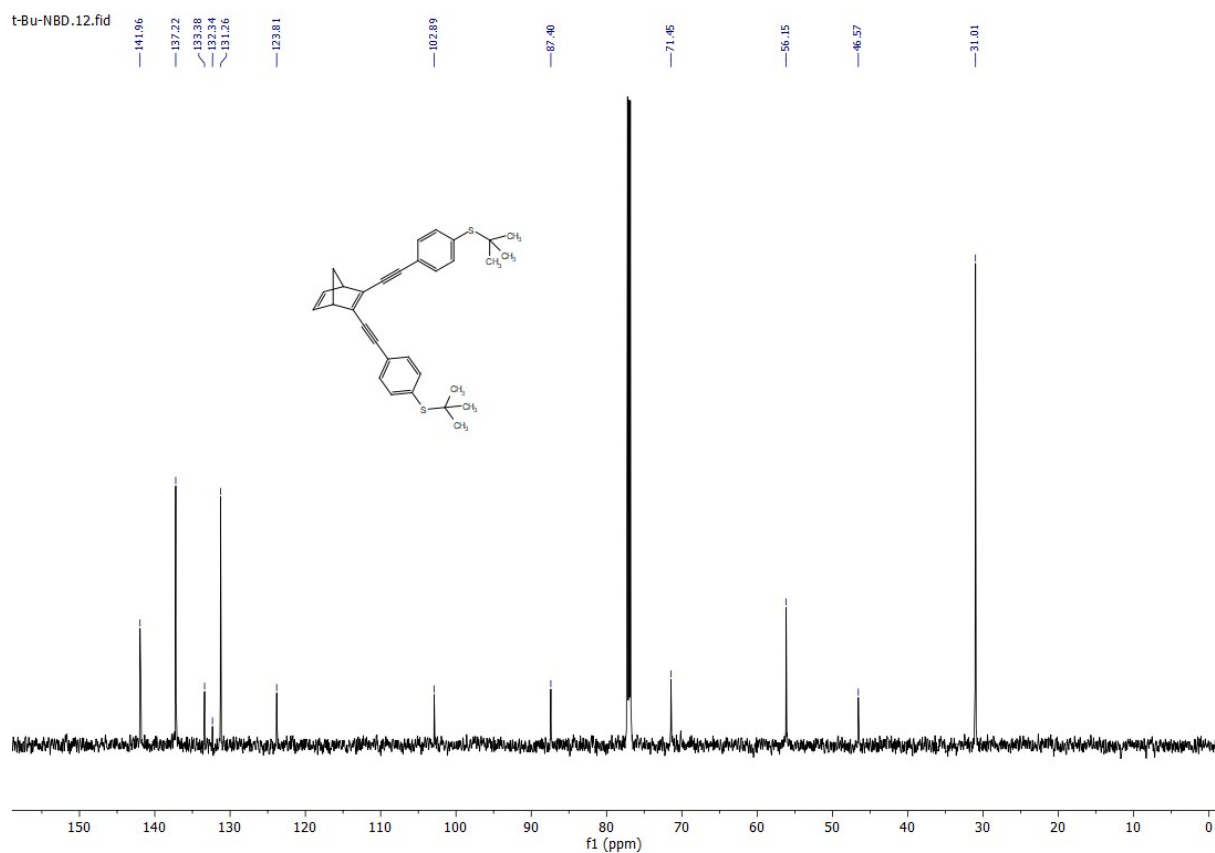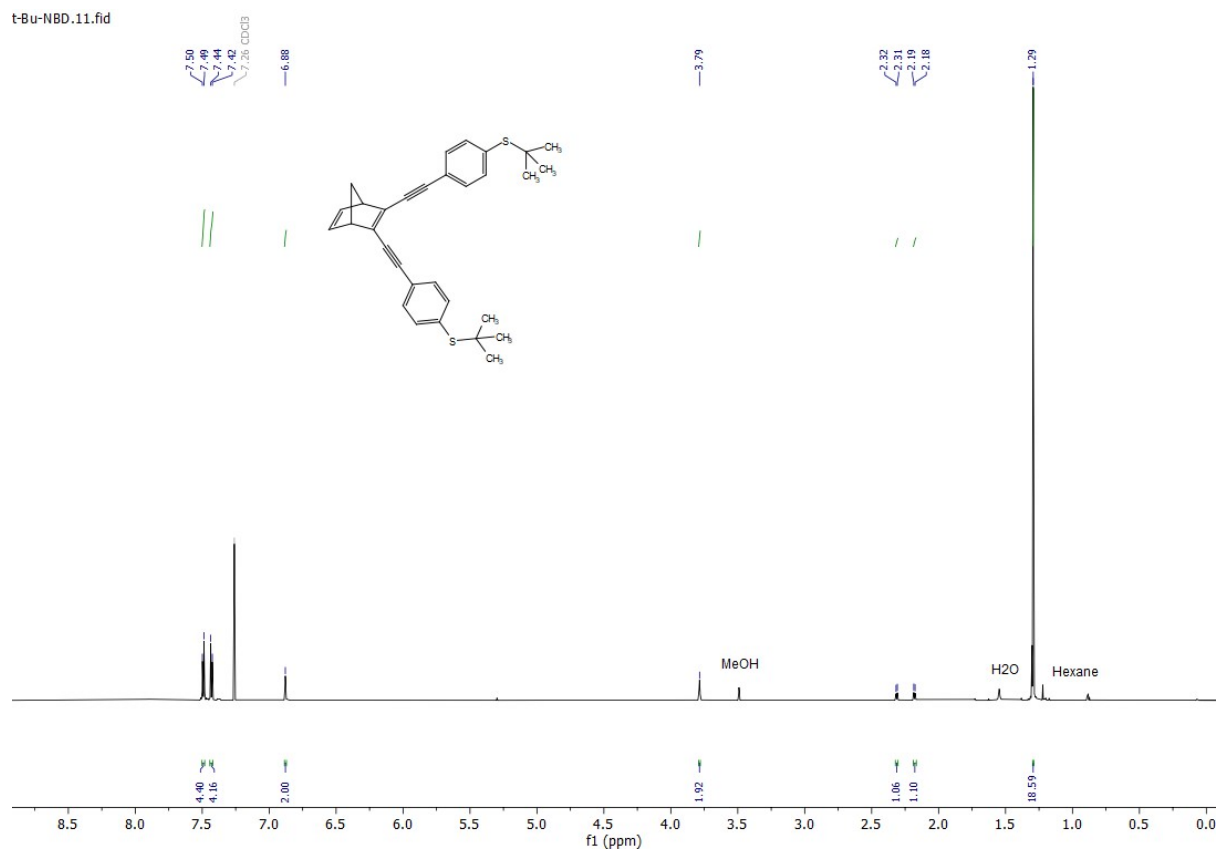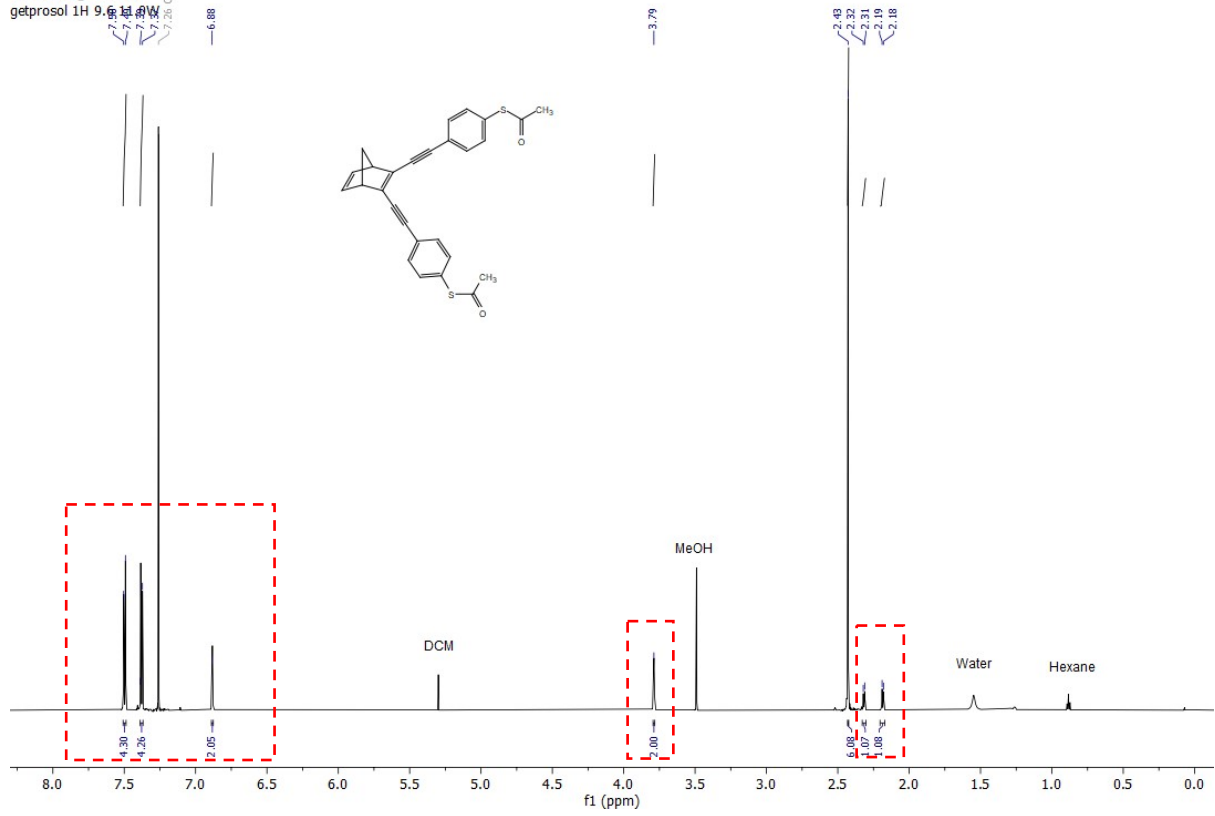
Fig. S1. ^{1}H-NMR 700 MHz spectrum of **NBD-1** in CDCl$_3$.

Fig. S2. ^{13}C-NMR 700 MHz spectrum of **NBD-1** in CDCl$_3$.

8

—3.79

3.818 3.816 3.814 3.812 3.810 3.808 3.806 3.804 3.802 3.800 3.798 3.796 3.794 3.792 3.790 3.788 3.786 3.784 3.782 3.780 3.778 3.776 3.774 3.772
f1 (ppm)

—2.31

—2.19

—2.18

.33   2.32   2.31   2.30   2.29   2.28   2.27   2.26   2.25   2.24   2.23   2.22   2.21   2.20   2.19   2.18   2.17   2.16
f1 (ppm)
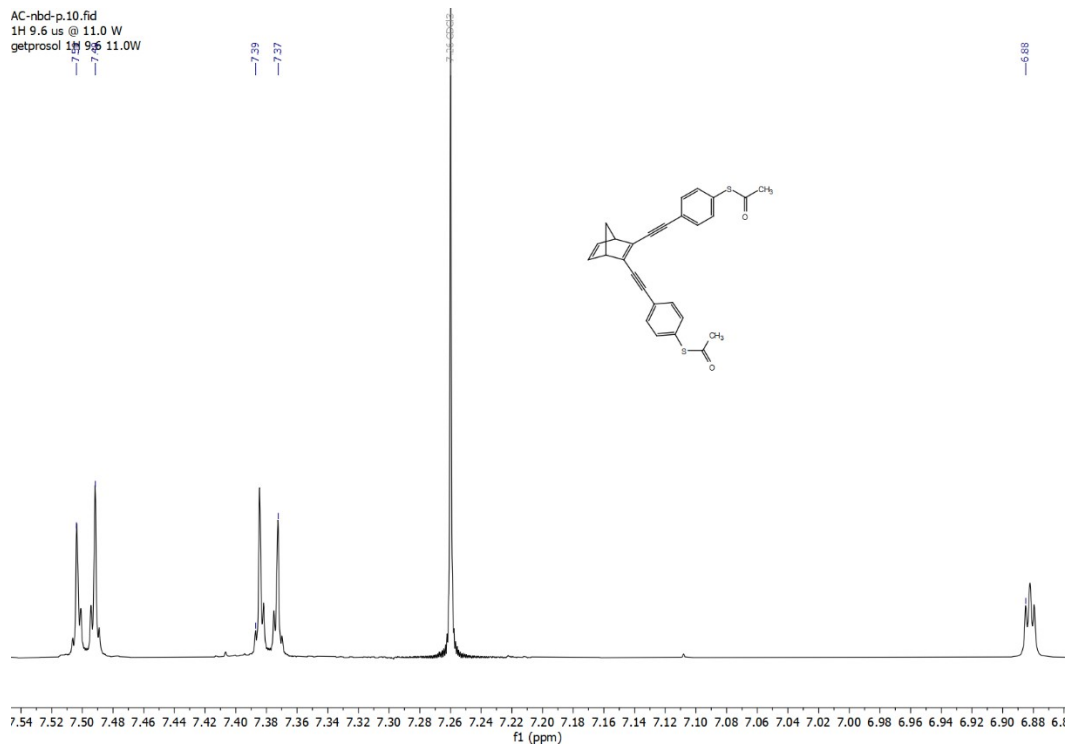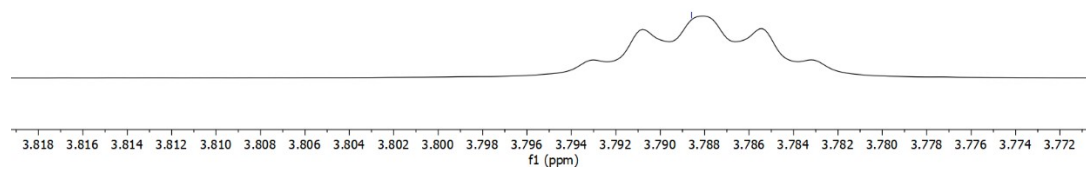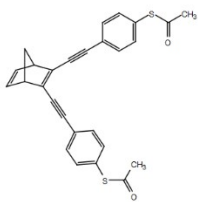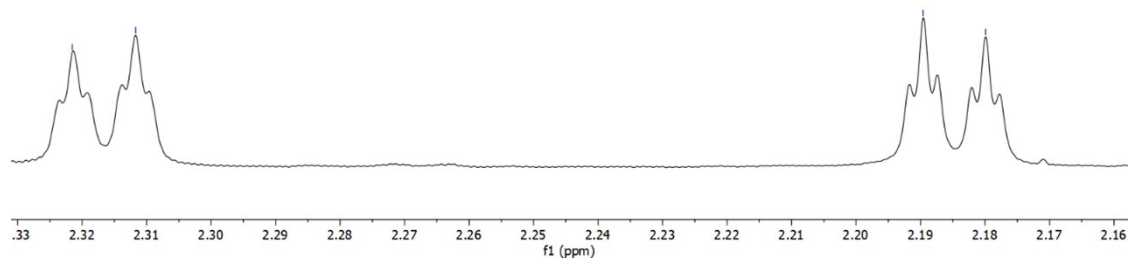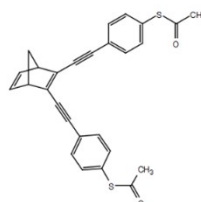
Fig. S3. ^{1}H-NMR 700 MHz spectrum of **NBD-2** and zoom in areas in different parts of spectrum in CDCl$_3$.
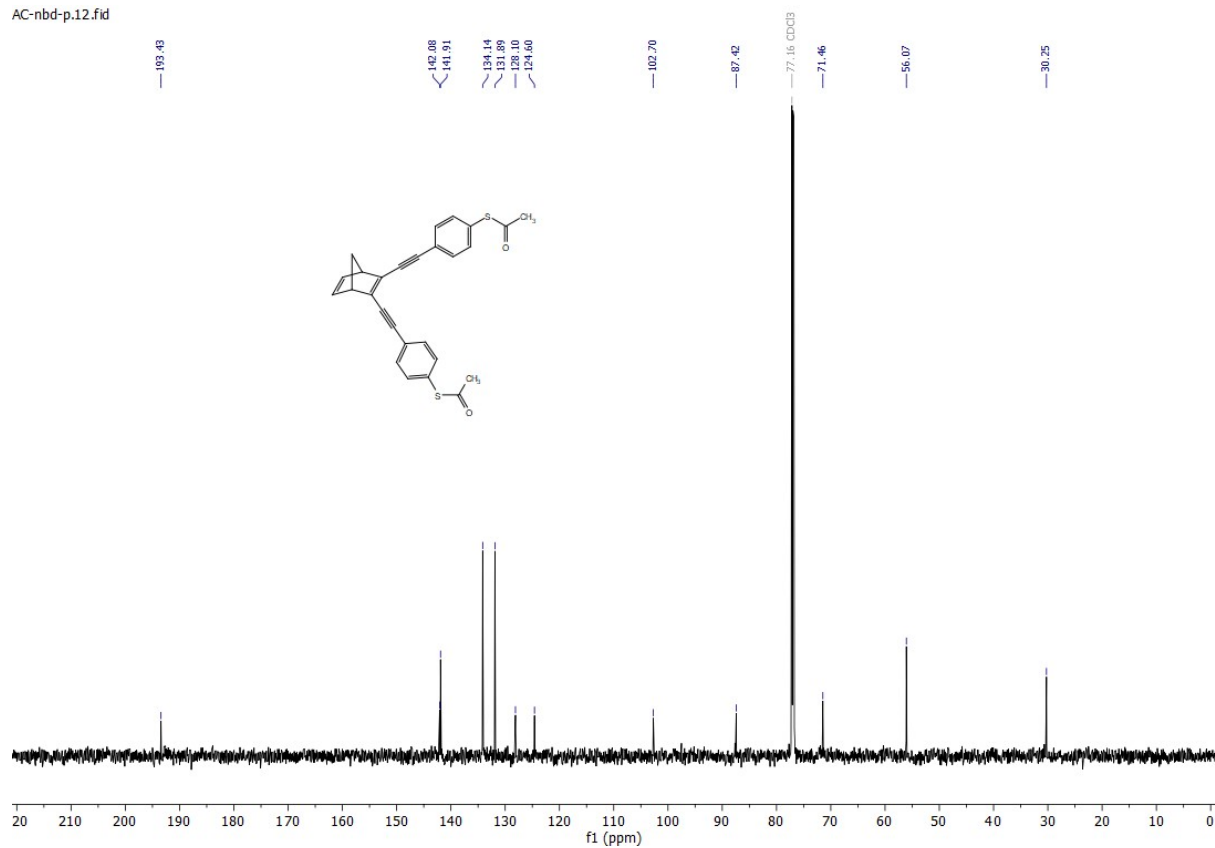
Fig. S4. ^{13}C-NMR 700 MHz spectrum of **NBD-2 in** CDCl$_3$.
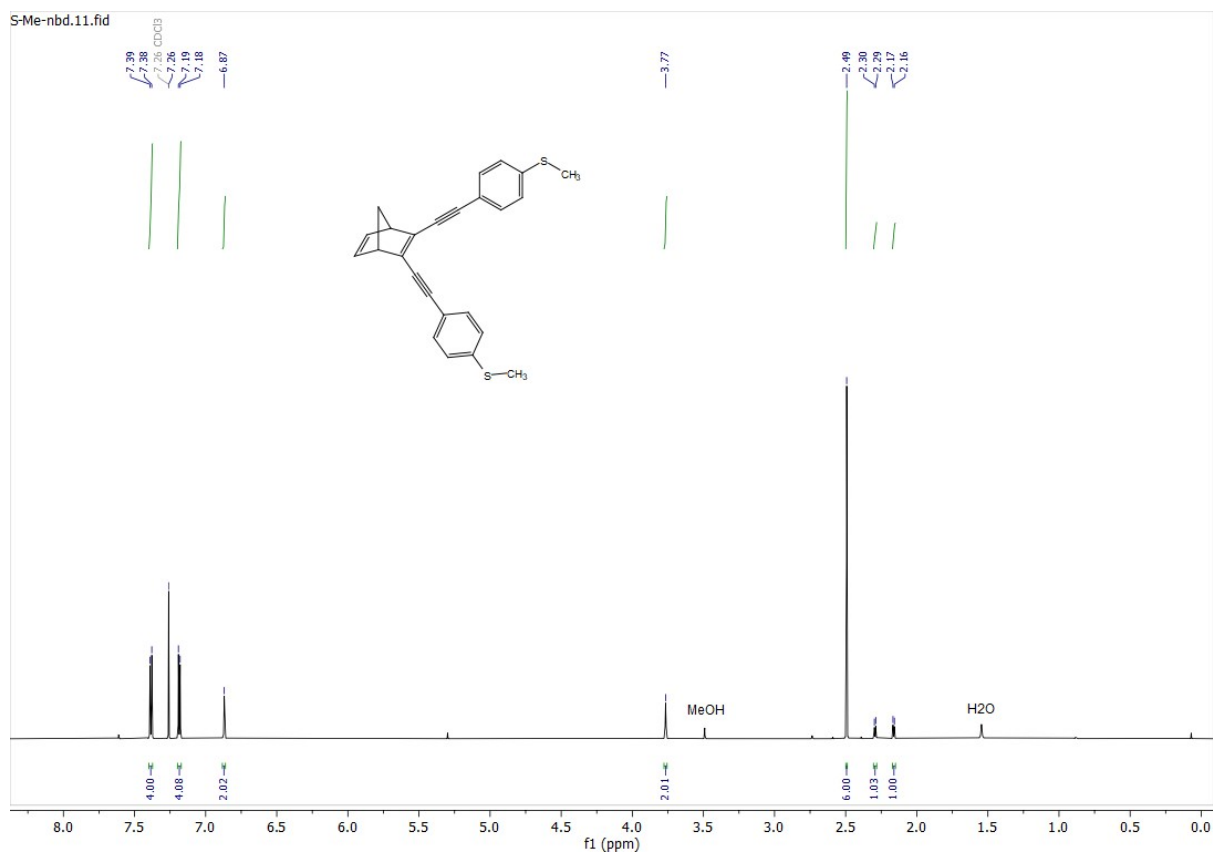
Fig. S5. ^{1}H-NMR 700 MHz spectrum of **NBD-3** in CDCl$_3$.

Fig. S6. ^{13}C-NMR 700 MHz spectrum of **NBD-3 in** CDCl$_3$.

#	m/z	I	I %
1	491.1814	108474	100.0
2	492.1843	35385	32.6
3	493.1803	14822	13.7
4	494.1847	3890	3.6

C31H32S2, M+nNa, 491.1838

Distribució isotòpica teòrica prevista

#	m/z	I	I %
1	491.1838	1026	100.0
2	492.1870	364	35.5
3	493.1839	154	15.1
4	494.1847	38	3.7
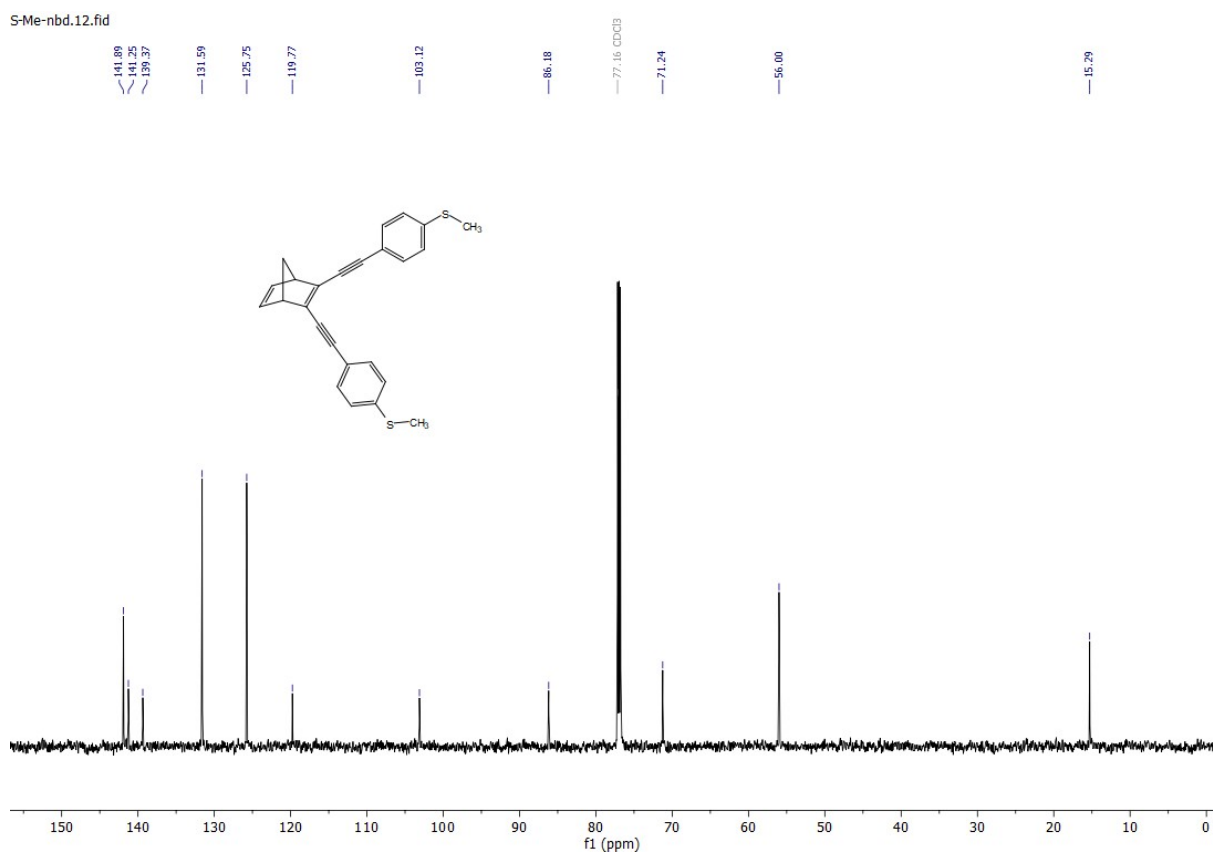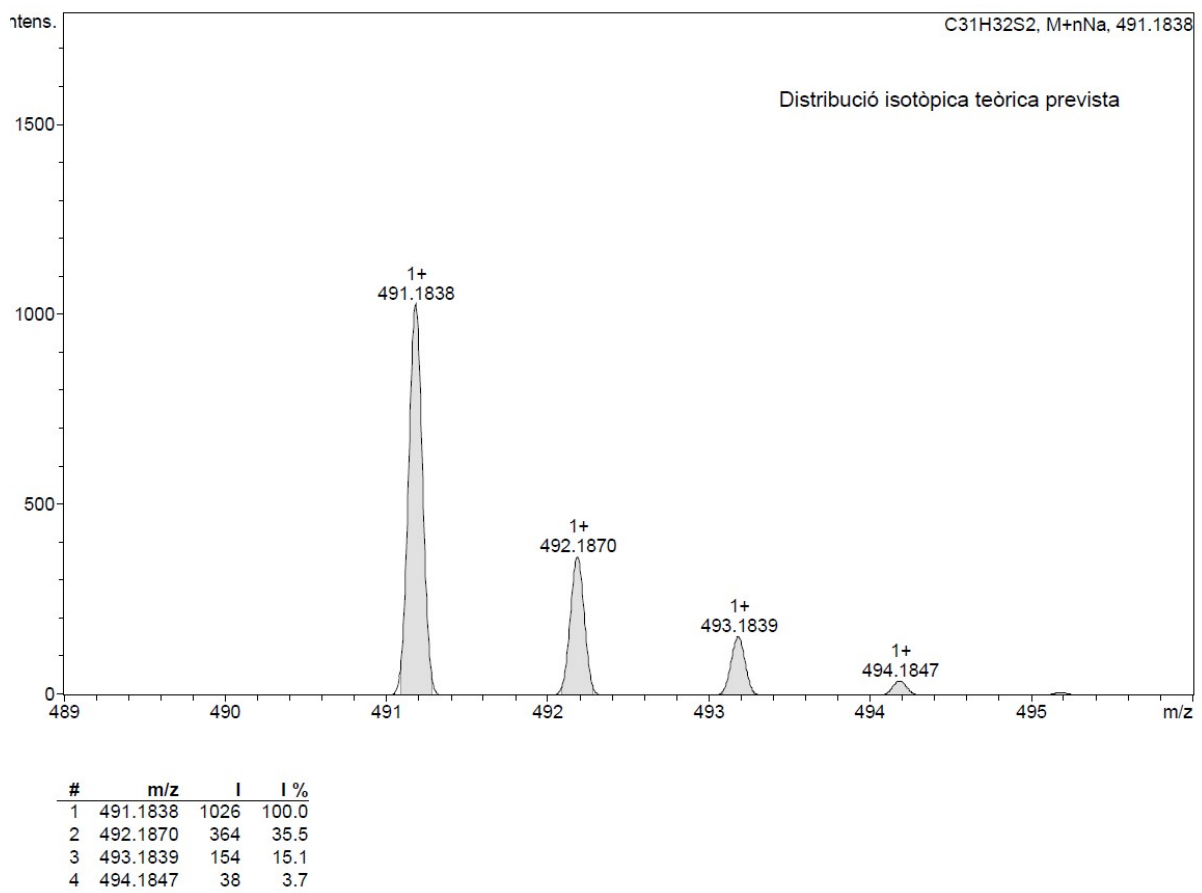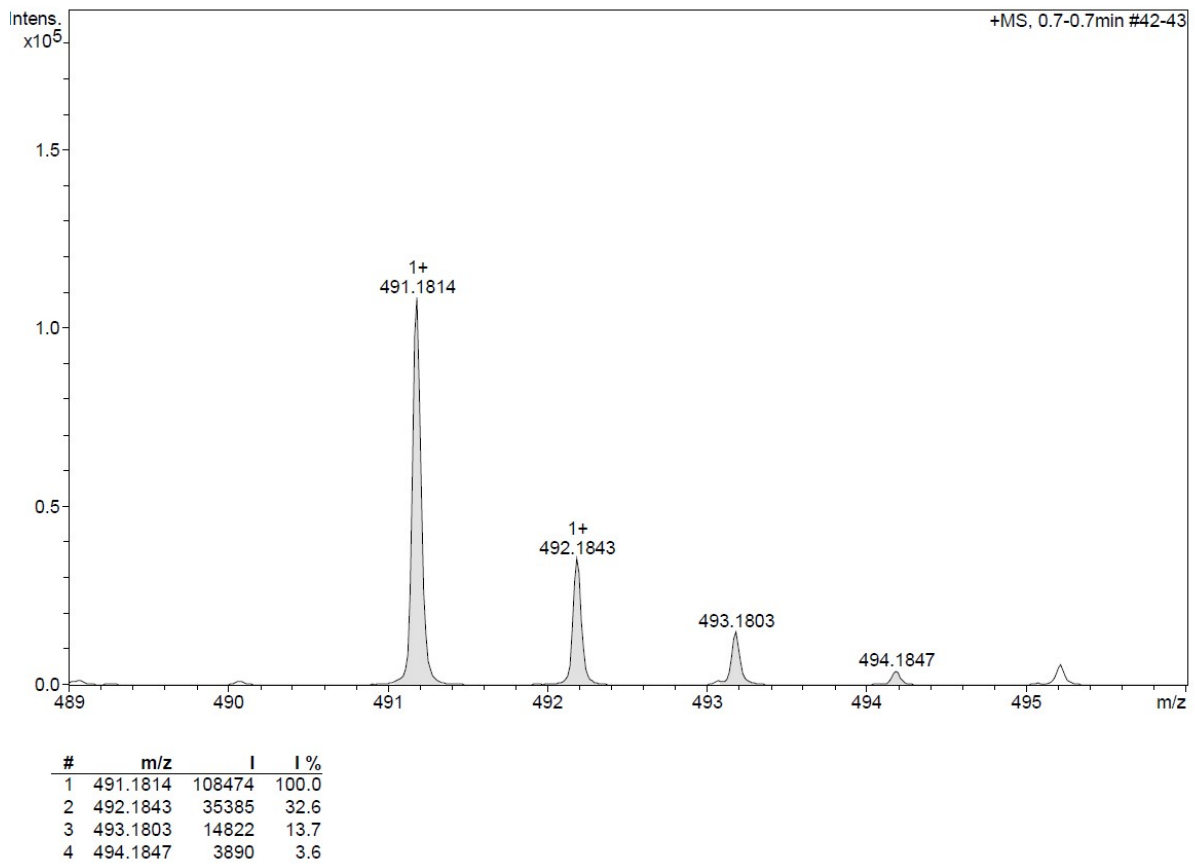
Fig. S7. HRMS of **NBD-1**.
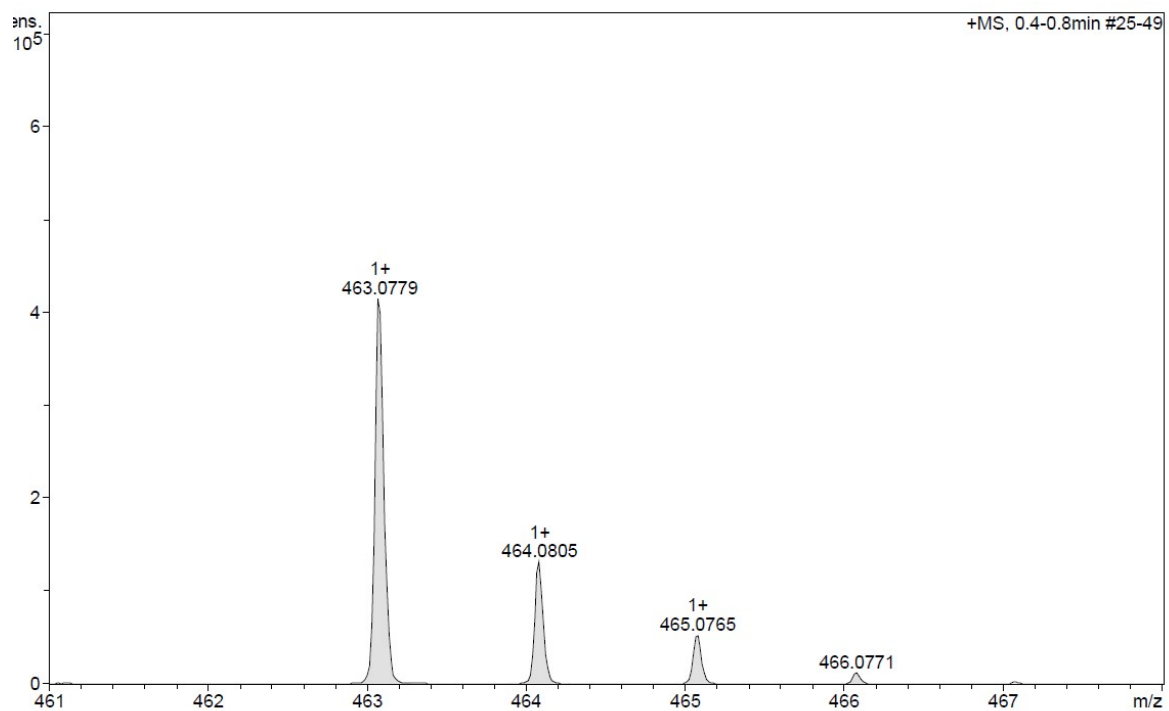
#	m/z	I	I %
1	463.0779	414294	100.0
2	464.0805	131802	31.8
3	465.0765	52692	12.7
4	466.0771	12169	2.9

C27H20O2S2, M+nNa, 463.0797

Distribució isotòpica teòrica prevista
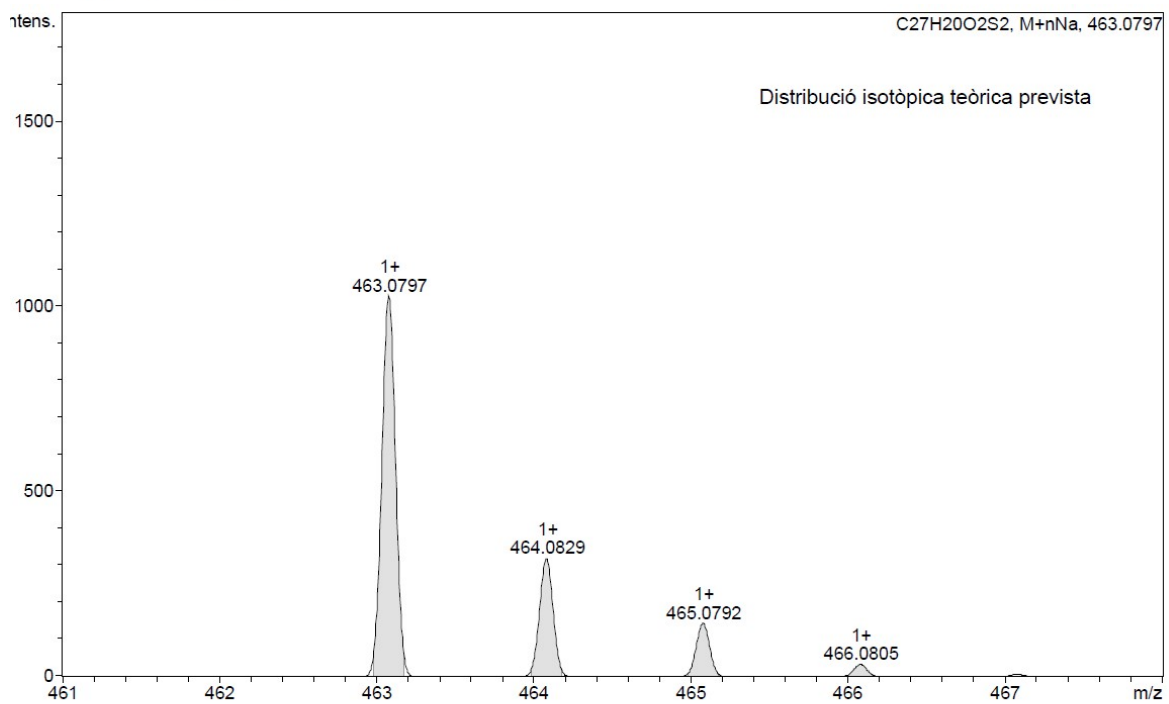
#	m/z	I	I %
1	463.0797	1026	100.0
2	464.0829	318	31.0
3	465.0792	144	14.0
4	466.0805	33	3.2

Fig. S8. HRMS of **NBD-2**.

14

Intens.
x10^5

1+
407.0880

1+
408.0904

1+
409.0855

410.0847

#	m/z	I	I %
1	407.0880	149949	100.0
2	408.0904	40803	27.2
3	409.0855	16931	11.3
4	410.0847	3851	2.6

Intens.

C25H20S2, M+nNa, 407.0899

Distribució isotòpica teòrica prevista

1+
407.0899

1+
408.0930

1+
409.0889

1+
410.0902

#	m/z	I	I %
1	407.0899	1026	100.0
2	408.0930	296	28.8
3	409.0889	133	13.0
4	410.0902	29	2.8
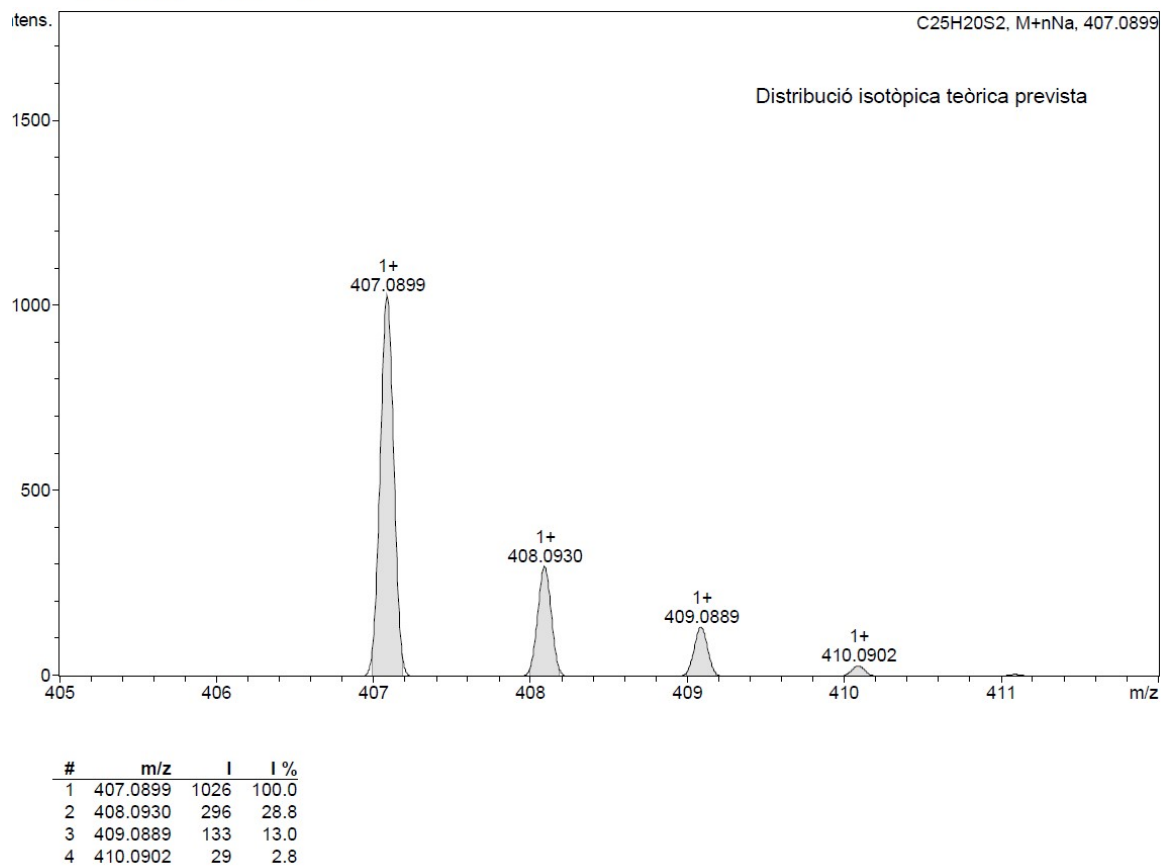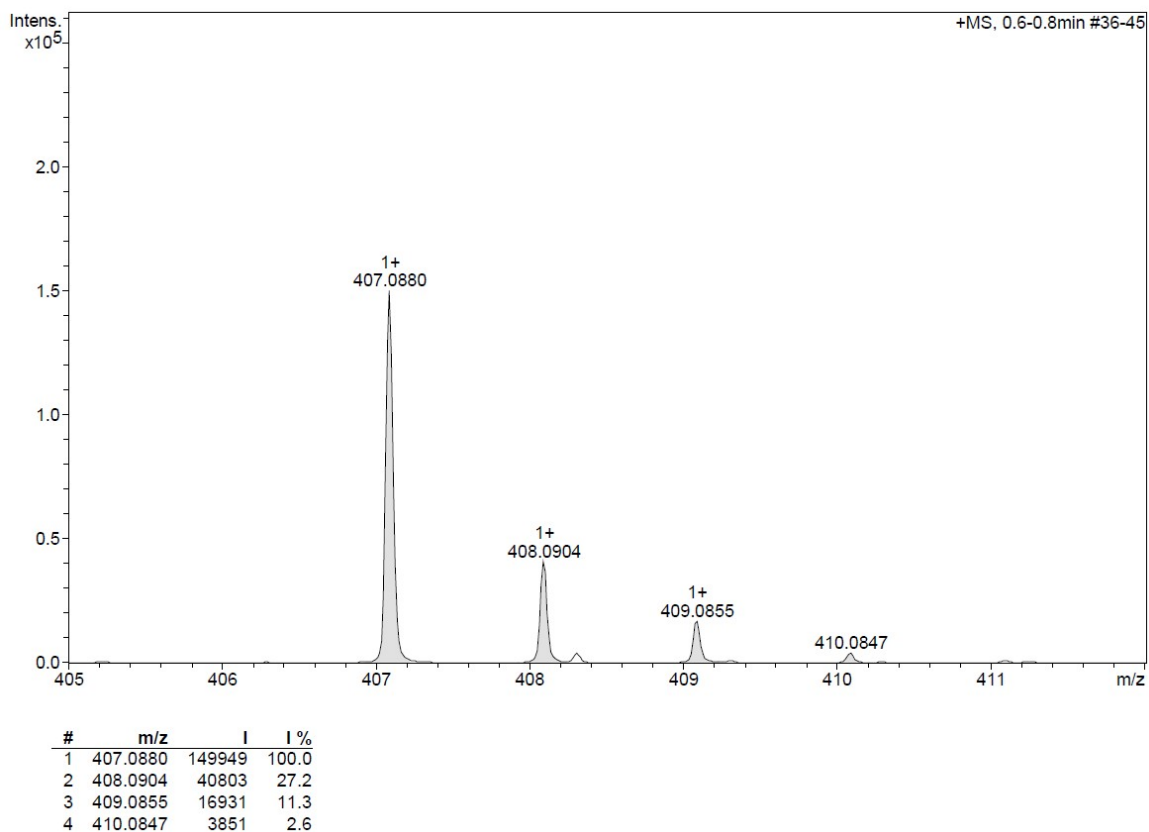
Fig. S9. HRMS of **NBD-3**.

2. Single-crystal X-ray diffraction measurements

NBD-2 crystals were grown in a mixture of dichloromethane and hexane (2:10). A crystal with suitable dimensions, measuring $0.03 \times 0.08 \times 0.12$ mm³, was carefully chosen and mounted on a Rigaku XtaLAB Synergy-R diffractometer. The diffractometer was equipped with a Cu Kα X-ray ($\lambda = 1.542$ Å) source and a HyPix detector. The measurements were conducted at a fixed temperature of 112(2) K, employing Ω scans and a rotating-anode X-ray source with a rotation rate of 0.5 degrees per frame. The indexing of the diffraction pattern and determination of the optimal number of runs and images were carried out based on the strategy calculation using the CrysAlis Pro program (version 1.171.42.79a). Subsequently, the unit cell parameters were refined.

Data reduction, scaling, and absorption correction were also performed using CrysAlis Pro. To correct for absorption effects, a Gaussian absorption correction was applied. The absorption correction procedure involved Gaussian integration over a multifaceted crystal model, and an empirical absorption correction was also employed using spherical harmonics implemented in the SCALE3 ABSPACK scaling algorithm. The crystal structure was initially solved by intrinsic phasing using the SHELXT program,[5] followed by subsequent structure refinements using SHELXL.[5]

Compound	NDB-2
Formula	$C_{27}H_{20}O_2S_2$
$Dcalc$ / g cm^{-3}	1.325
μ/mm^{-1}	2.352
Formula Weight	440.55
Colour	yellow
Shape	plate
Size/mm³	$0.026 \times 0.078 \times 0.123$
T/K	112(2)
Crystal System	monoclinic
Space Group	$P2_1/c$
a/Å	19.8077(4)
b/Å	5.69090(10)
c/Å	20.2663(5)
α degree	90
β degree	104.820(2)
γ degree	90
V/Å³	2208.50(8)
Z	4
Z'	1
Wavelength/Å	1.54184
Radiation type	Cu K$_\alpha$
Θ min/°	2.307
Θ max/°	75.632
Measured Refl.	21637
Independent Refl.	4413
Reflections with I > 2(I)	3922
Rint	0.0266
Parameters	282
Restraints	0
Largest Peak	0.499

Deepest Hole	-0.291
Goodness of fit	1.063
wR_2 (all data)	0.1021
wR_2	0.0963
R_1 (all data)	0.0401
R_1	0.0351

Anisotropic refinement was applied to all non-hydrogen atoms, enabling a comprehensive analysis of their thermal motion. The positions of hydrogen atoms were determined geometrically and refined using the riding model, ensuring their precise placement within the crystal structure.

Crystal data:

The crystallographic data has been deposited with the Cambridge Crystallographic Data Centre (CCDC) under the Deposition Number 2269540.
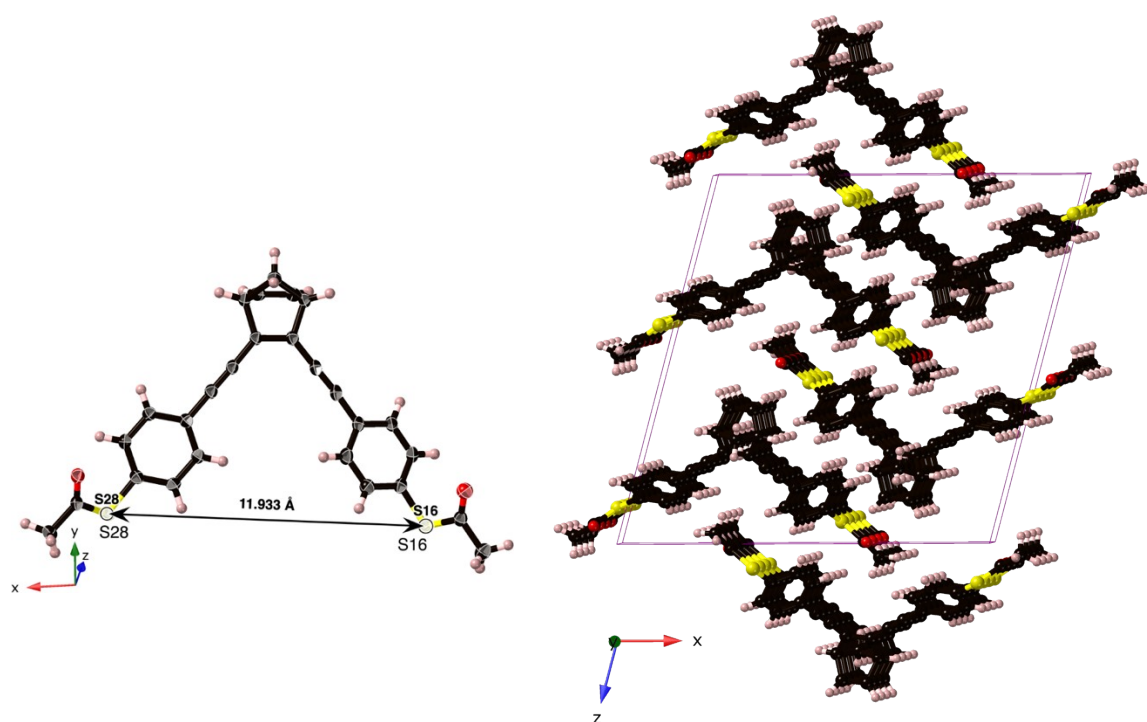
Fig. S10. (Left) Crystal structure of **NBD-2**, highlighting the molecular unit (which is also the asymmetric unit). Displacement ellipsoids are depicted at a 50% probability level. (Right) Packing along the *y*-axis.
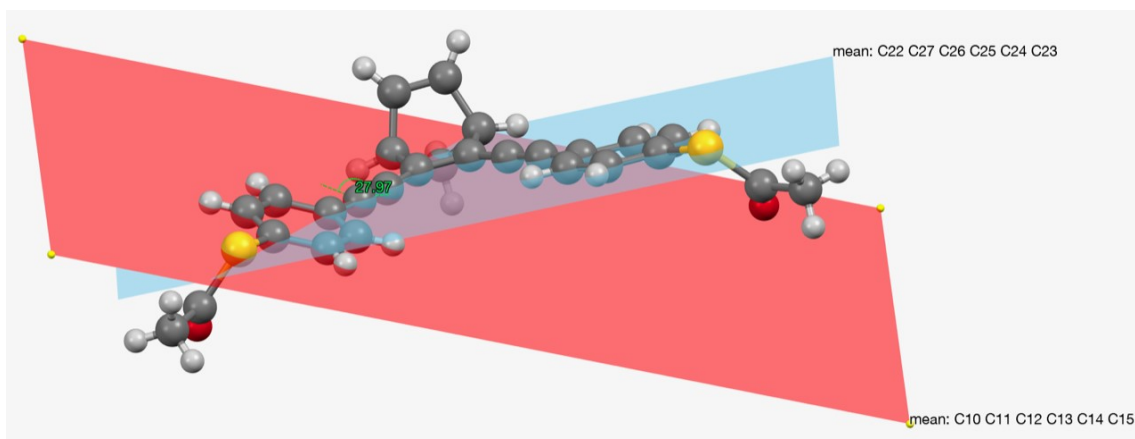
Fig. S11. Planes and angles of the two arms in the **NBD-2** crystal structure.

3. Mechanically controllable break junction measurements

The experimental setup consisted of a flexible phosphor bronze substrate with a lithographically defined gold nanowire. The sample was mounted in a three-point bending setup, enabling controlled movement through a piezo-electric actuator. As the sample was bent, the gold wire stretched and broke, forming nanometric-sized electrodes for molecule anchoring. During the MCBJ experiments, the current flowing through the wire was measured at a fixed bias while increasing the displacement between the gold electrodes, resulting in breaking traces that depicted the conductance versus electrode displacement curves. An empty junction exhibited an exponential decay pattern, indicative of tunnelling through a fixed-height barrier. Conversely, the presence of a molecule in the junction produced a molecular conductance plateau, in which the conductance of the junction remained relatively constant with increasing electrode displacement. Further displacement caused the molecule to disconnect from the electrodes, resulting in a read-out drop below the noise floor of the measurement setup. The cycle could be restarted by pushing the electrodes back together. Thousands of breaking-making cycles were recorded for each experiment to ensure robust data collection.[6, 7]

The histograms and fitting results obtained from the measurements conducted in this study are presented in the following.

The raw data was processed as follows: Initially, a trained neural network was employed to identify and separate the traces that did not contain molecular plateaus (referred to as "empty" traces) from the remaining data. The methodology for this separation is briefly described in previously published work,[8] and a detailed account will be presented in a forthcoming publication. Subsequently, the remaining

molecular traces were classified into distinct classes using the *k*-means++ algorithm, following the procedure outlined in the literature.[9] The feature space used for classification consisted of a 30×30 binned two-dimensional histogram constructed using a displacement range of 0 to 2 nm and a conductance range of -0.5 to -6 $\log(G/G_0)$. Additionally, a one-dimensional histogram with 100 bins in the conductance range of -0.5 to -6 $\log(G/G_0)$ was appended to the feature space.

It should be noted that the small peak observed around 1×10^{-6} G_0 is an artifact of the measurement electronics and is primarily present in the "empty" traces.
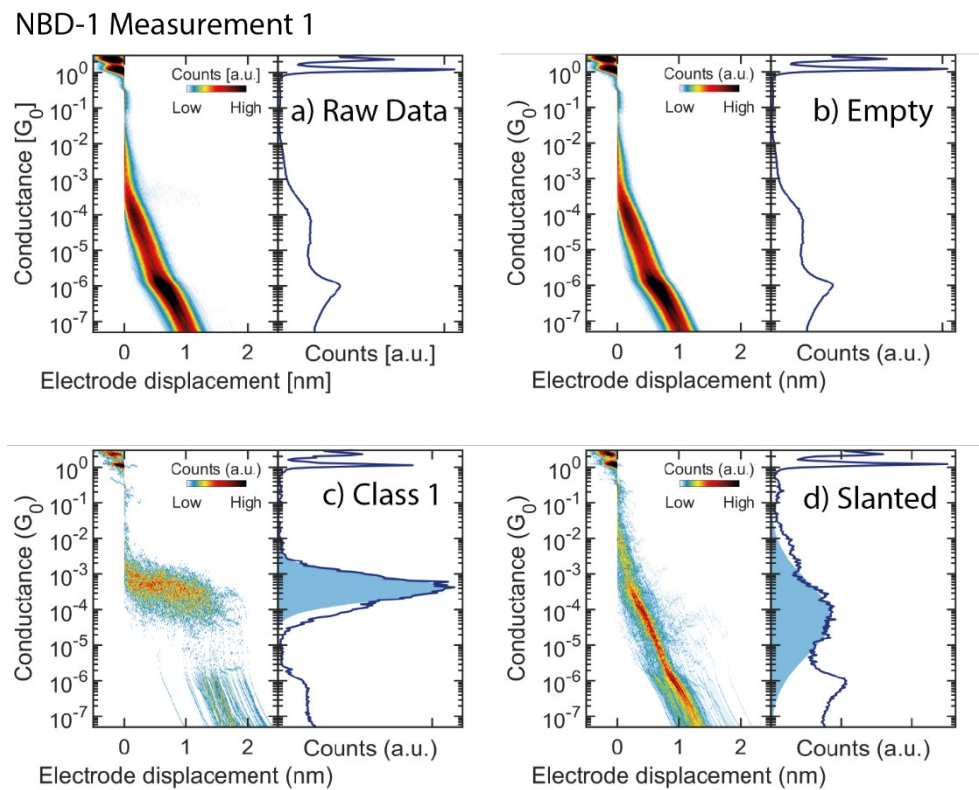
Fig. S12. Two-dimensional (left) and one-dimensional (right) histograms of (a) the raw data, (b) the removed empty traces, (c) Class 1, and (d) Class 2, obtained from the first **NBD-1** measurement.
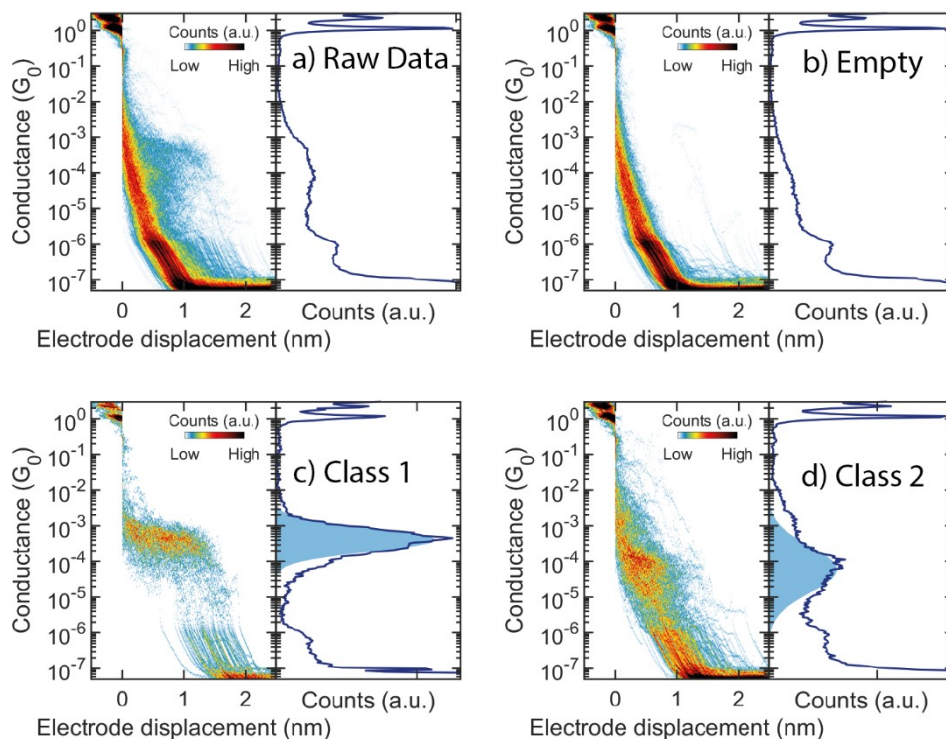
Fig. S13. Two-dimensional (left) and one-dimensional (right) histograms of (a) the raw data, (b) the removed empty traces, (c) Class 1, and (d) Class 2, obtained from the second **NBD-1** measurement.
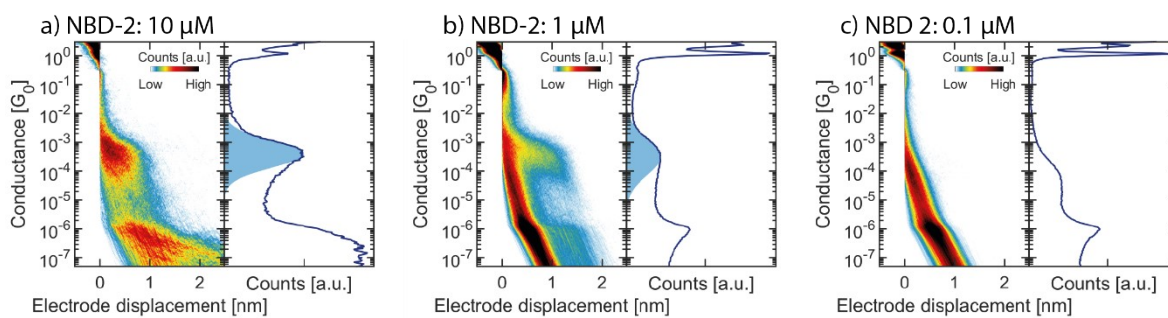
Fig. S14. Two-dimensional (left) and one-dimensional (right) histograms of the raw data of **NBD-2** with a concentration of (a) 10 µM, (b) 1 µM, and (c) 0.1 µM.
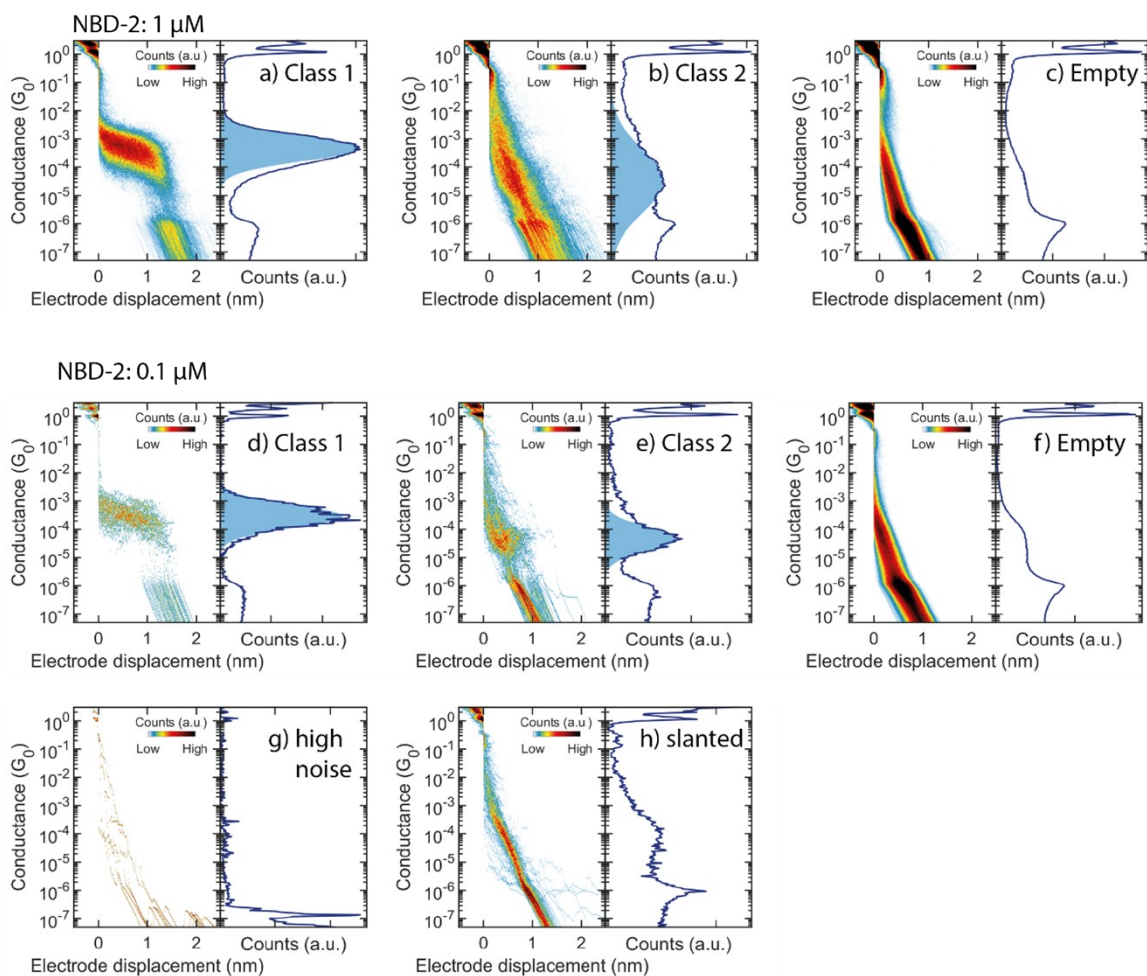
Fig. S15. Two-dimensional (left) and one-dimensional (right) histograms of (a) Class 1, (b) Class 2, and (c) the empty traces, obtained from the **NBD-2** measurement at 1 μM. Histograms (d), (e), and (f) are obtained using a concentration of 0.1 μM, from which two additional classes are observed: (g) one that shows a few outlier traces with high noise and (h) one that contains slanted traces. The two additional classes are excluded from the main analysis as they do not contain any molecular plateaus.

NBD-3 Measurement 1
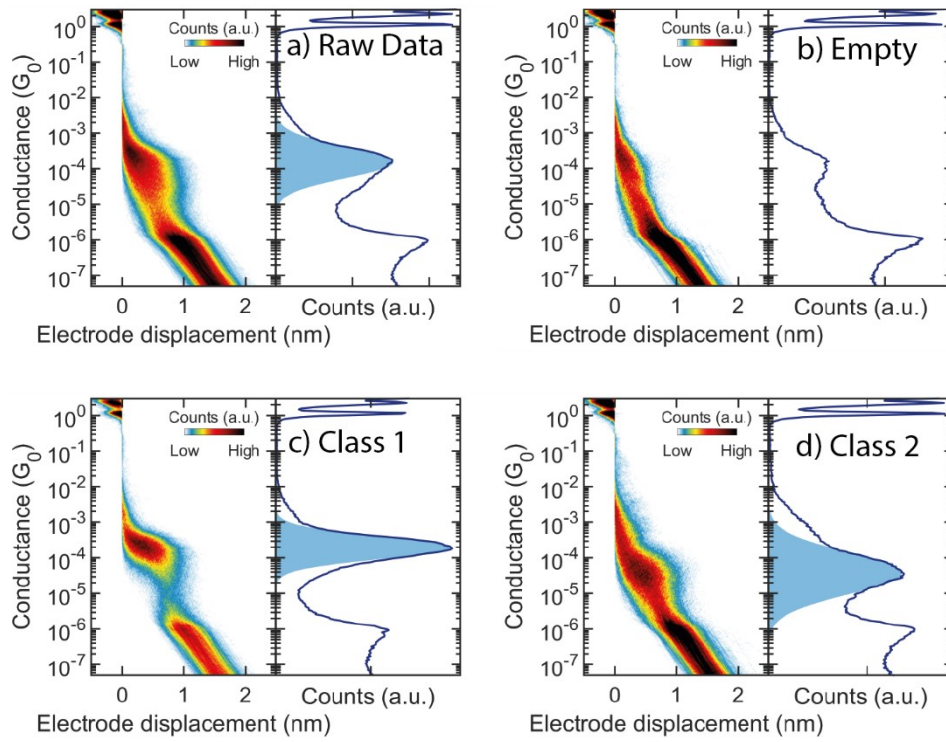
Fig. S16. Two-dimensional (left) and one-dimensional (right) histograms of (a) the raw data, (b) the empty traces, (c) Class 1, and (d) Class 2, obtained from the first **NBD-3** measurement.

NBD-3 Measurement 2
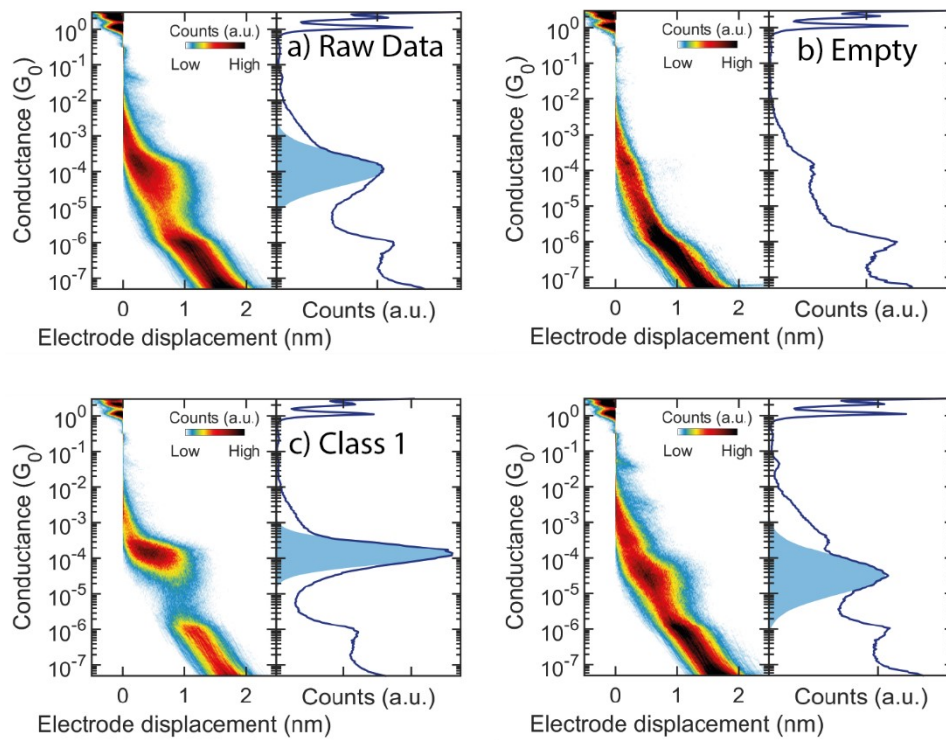
Fig. S17. Two-dimensional (left) and one-dimensional (right) histograms of (a) the raw data, (b) the empty traces, (c) Class 1, and (d) Class 2, obtained from the second **NBD-3** measurement.

Table S1. Tabulated summarization of the MCBJ measurement data presented in this work, including extracted conductance values for the classes obtained by clustering.

Molecule	Measurement	Concentration (µM)	Voltage Bias (V)	N traces	Class 1 Yield (%)	Class 1 G/G_0	Class 1 length (nm)	Class 2 Yield (%)	Class 2 G/G_0
NBD-1	1	1	0.1	10000	1	4.0×10^{-4}	1.3	//	//
	2	1	0.1	1380	7	4.1×10^{-4}	1.3	9	9.2×10^{-5}
NBD-2	1	10	0.1	2321	//	//	//	//	//
	2	1	0.1	10000	11	4.7×10^{-4}	1.2	14	3.3×10^{-5}
	3	0.1	0.1	10000	0.4	2.9×10^{-4}	1.2	14	4.7×10^{-5}
NBD-3	1	1	0.1	10000	32	2.0×10^{-4}	0.7	40	3.7×10^{-5}
	2	1	0.1	10000	29	1.4×10^{-4}	1.0	49	3.2×10^{-5}

4. Electron transport calculations

The three NBD structures and the two QC structures were optimized in vacuum prior to the electron transport calculations. This was achieved using the PBE0[10-13] functional in conjunction with the cc-pVDZ[14, 15] basis set in Gaussian 16.[16] For calculating the electronic transmission, the PBE[10] functional was employed along with a double-ζ basis set including polarization (DZP), implemented in the grid-based projector augmented wave (GPAW) electronic structure code[17, 18] for all atoms.

The transmission functions were computed using a non-equilibrium Green's function (NEGF) approach within a Landauer-Büttiker picture combined with density functional theory (DFT),[19-25] implemented in the Atomic Simulation Environment (ASE)[26] and GPAW. The molecules were positioned in an Au-molecule-Au junction, where the anchoring groups were connected to the electrodes via tetrahedral gold tips on the surface of 4×4 Au(111) surfaces. Periodic boundary conditions were applied in the plane of the surfaces. The molecules underwent relaxation within the junction, employing a force threshold of 0.05 eV Å^{-1}, while all the gold atoms were kept fixed. To calculate the transmission, k-point sampling was conducted over a $2 \times 2 \times 1$ Monkhorst-Pack mesh in the first Brillouin zone.

5. References

1.   A. Lennartson, M. Quant and K. Moth-Poulsen, *Synlett*, 2015, **26**, 1501-1504.
2.   T. Pinault, F. Chérioux, B. Therrien and G. Süss-Fink, *Heteroatom Chemistry: An International Journal of Main Group Elements*, 2004, **15**, 121-126.
3.   E. H. Van Dijk, D. J. Myles, M. H. Van Der Veen and J. C. Hummelen, *Organic Letters*, 2006, **8**, 2333-2336.
4.   J. Hu, X. Deng, H. Zhang, Y. Diao, S. Cheng, S.-L. Zheng, W.-M. Liao, J. He and Z. Xu, *Inorganic Chemistry*, 2020, **60**, 161-166.
5.   G. M. Sheldrick, *Acta Crystallographica Section A: Foundations and Advances*, 2015, **71**, 3-8.
6.   H. Park, A. K. Lim, A. P. Alivisatos, J. Park and P. L. McEuen, *Applied Physics Letters*, 1999, **75**, 301-303.
7.   C. A. Martin, R. H. Smit, R. v. Egmond, H. S. van der Zant and J. M. van Ruitenbeek, *Review of Scientific Instruments*, 2011, **82**.
8.   A. Daaoub, L. Ornago, D. Vogel, P. Bastante, S. Sangtarash, M. Parmeggiani, J. Kamer, N. Agraït, M. Mayor and H. van der Zant, *The Journal of Physical Chemistry Letters*, 2022, **13**, 9156-9164.
9.   D. Cabosart, M. El Abbassi, D. Stefani, R. Frisenda, M. Calame, H. S. J. van der Zant and M. L. Perrin, *Applied Physics Letters*, 2019, **114**, 143102.
10.   J. P. Perdew, K. Burke and M. Ernzerhof, *Physical Review Letters*, 1996, **77**, 3865.
11.   J. P. Perdew, K. Burke and M. Ernzerhof, *Physical Review Letters*, 1998, **80**, 891.
12.   M. Ernzerhof and G. E. Scuseria, *The Journal of Chemical physics*, 1999, **110**, 5029-5036.
13.   C. Adamo and V. Barone, *The Journal of Chemical Physics*, 1999, **110**, 6158-6170.
14.   T. H. Dunning Jr, *The Journal of Chemical Physics*, 1989, **90**, 1007-1023.
15.   D. E. Woon and T. H. Dunning Jr, *The Journal of Chemical Physics*, 1993, **98**, 1358-1371.
16.   M. J. Frisch, G. W. Trucks, H. B. Schlegel *et al.*, Gaussian 16 Revision A.03, Gaussian Inc., Wallingford CT, 2016.
17.   J. J. Mortensen, L. B. Hansen and K. W. Jacobsen, *Physical Review B*, 2005, **71**, 035109.
18.   A. H. Larsen, M. Vanin, J. J. Mortensen, K. S. Thygesen and K. W. Jacobsen, *Physical Review B*, 2009, **80**, 195112.
19.   R. Landauer, *IBM Journal of Research and Development*, 1957, **1**, 223-231.
20.   R. Landauer, *Philosophical Magazine*, 1970, **21**, 863-867.
21.   C. Caroli, R. Combescot, P. Nozieres and D. Saint-James, *Journal of Physics C: Solid State Physics*, 1971, **4**, 916.
22.   Y. Meir and N. S. Wingreen, *Physical Review Letters*, 1992, **68**, 2512.
23.   M. Brandbyge, J.-L. Mozos, P. Ordejón, J. Taylor and K. Stokbro, *Physical Review B*, 2002, **65**, 165401.
24.   M. Strange, I. S. Kristensen, K. S. Thygesen and K. W. Jacobsen, *The Journal of Chemical Physics*, 2008, **128**.
25.   J. Chen, K. S. Thygesen and K. W. Jacobsen, *Physical Review B*, 2012, **85**, 155140.
26.   A. H. Larsen, J. J. Mortensen, J. Blomqvist, I. E. Castelli, R. Christensen, M. Dułak, J. Friis, M. N. Groves, B. Hammer and C. Hargus, *Journal of Physics: Condensed Matter*, 2017, **29**, 273002.